Research Square

Preprints are preliminary reports that have not undergone peer review.
They should not be considered conclusive, used to inform clinical practice,
or referenced by the media as validated information.

Rock burst prevention and control method for irregular section coal pillars under thick hard roof with multiple mining disturbances

Fei Gao
Chongqing University
Jie Chen
Chongqing University
Chuanjiu Zhang
Chongqing University
Kaiwen Shi
Chongqing University
Xiaobo Hao
Chongqing University
Li Zhang
Chongqing University
Xiang Ma
Chongqing University
Haiyong Hu
Chongqing University
Dafa Yin
Chongqing University
Wenxin Dong
dongwenxin@cqu.edu.cn
Chongqing University

Article

Keywords: irregular coal pillars, thick and hard roof, rock burst risk, coal pillar stress, prevention and control of rock burst

Posted Date: June 23rd, 2026

DOI: https://doi.org/10.21203/rs.3.rs-9959843/v1

License: This work is licensed under a Creative Commons Attribution 4.0 International License.
Read Full License

Additional Declarations: No competing interests reported.

Rock burst prevention and control method for irregular section coal pillars under thick hard roof with multiple mining disturbances

Fei Gao[1,2], Jie Chen[1,2], Chuanjiu Zhang[1,2], Kaiwen Shi[1,2], Xiaobo Hao[1,2], Li Zhang[1,2], Xiang Ma[1,2], Haiyong Hu[1,2], Dafa Yin[1,2], Wenxin Dong[1,2,3,4]

[1] School of Resources and Safety Engineering, Chongqing University, Chongqing 400044, China; [2] State Key Laboratory of Coal Mine Disaster Dynamics and Control, Chongqing University, Chongqing 400044, China;[3] Jinsha Mining Technology (Chongqing) Co., Ltd., Chongqing 400074, China;[4] Chongqing University Industrial Technology Research Institute, Chongqing 401329, China

* Corresponding author: dongwenxin@cqu.edu.cn

Abstract: Regarding the prevention and control of rock bursts in irregular coal pillars in thick coal seams, with the No. 5316 working face of Shandong Mine as the engineering background, a combination of on-site investigation, theoretical analysis, numerical simulation and on-site industrial tests was adopted to systematically study the stress and impact instability evolution law of irregular coal pillars in working faces with thick and hard roofs. The rock burst risk in the irregular coal pillar area under mining influence was systematically evaluated, and a coal pillar rock burst prevention and control method coordinating overlying strata structure optimization and stress control was proposed. The results show that the expressions of vertical stress and horizontal stress borne by coal pillars with different widths are derived, and the evolution law of stress in irregular coal pillars is studied through examples; the stability of irregular coal pillars under mining disturbance is systematically analyzed, and the energy-induced mechanism of impact instability of coal pillars is discussed and analyzed. Based on the Dempster-Shafer evidence Theory, an overall evaluation method for coal pillar rock burst risk is proposed, which integrates monitoring information from microseismic, online stress and drill cuttings methods within the same time window, and the early warning values for rock burst risk in irregular coal pillars are determined. In combination with the characteristics of rock burst risk areas in irregular coal pillars, a coal pillar rock burst prevention and control method that coordinates the optimization of overlying strata structure of thick and hard roof with stress control is proposed. The results of on-site industrial tests show that after the implementation of comprehensive prevention and control measures, there were no abnormal conditions in stress and working resistance of hydraulic supports in the irregular coal pillar area during the mining process of the working face. The rock burst prevention and control effect is good, which ensures the safe and efficient mining of the working face.

Key words: irregular coal pillars; thick and hard roof; rock burst risk; coal pillar stress; prevention and control

of rock burst

1 Introduction

Coal is an important energy source driving the development of the national economy. With the rapid development of China's economy, the status of coal as the main energy source will not change for a fairly long period of time[1,2]. At present, resources in eastern mines are depleted, and it has become imperative to recover a large number of residual coal pillars or main roadway coal pillars. However, since most of the surrounding working faces have been mined out, during the recovery process, the problem of multiple mining disturbances will inevitably be encountered. Moreover, with the increase in coal mining intensity and depth, coal mining conditions have become extremely complex, which can easily induce typical dynamic disasters such as rock bursts under mining disturbances. This is particularly true for thick coal seams, where rock burst disasters are becoming increasingly prominent. The particularity of thick coal seam mining determines that the overlying strata movement and surrounding rock stress distribution characteristics during the working face mining period are more complex than those of conventional working faces. Numerous experts and scholars at home and abroad have carried out extensive research on the movement law of overlying strata, the occurrence mechanism of rock bursts and their prevention and control technologies in thick coal seam working face mining, and have achieved a series of research results. In terms of the law of overlying strata movement, foreign scholars have successively put forward the "cantilever beam hypothesis", "pressure arch hypothesis", "pre-existing fracture hypothesis" and "articulated rock block hypothesis", which constitute the classic theoretical framework for the law of overlying strata movement in stope and provide a direction and scientific basis for the development of overlying strata theory in China. Therefore, the "transferred rock beam theory" [4], "masonry beam theory" [5], and "key stratum theory" [6] have been successively proposed and widely applied. Jiang Fuxing [7]proposed the stope overlying strata spatial structures under the mining boundary conditions of the working face, namely the "O"-shaped spatial structure, "θ"-shaped spatial structure, "C"-shaped spatial structure and "S"-shaped spatial structure, and studied the mine pressure laws under different spatial structures. Dou Linming[8] classified the overlying strata spatial structures into three types, namely OX, F and T types, according to the different boundary states of the overlying strata above the working face, and selected typical working faces representing each overlying strata structure to analyze the distribution law of seismic sources during the mining process. The above research results have formed a relatively complete law of overlying strata movement in working faces, providing a

foundation for the subsequent research and development of mine pressure and rock strata control theories[9-14]. In terms of the mechanism of rock burst occurrence, scholars at home and abroad have combined laboratory tests with engineering practices and put forward a series of important theories[15-22], such as the Strength Theory, Stiffness Theory, Energy Theory, Instability Theory and Catastrophe Theory. Dou Linming et al.[23] proposed the mechanism of rock burst induced by the superposition of dynamic and static loads, and studied the basic principles and specific measures for the prevention and control of coal seam rock bursts. Li Xibing et al. [24] revealed the essence of rock burst under the combined action of static load and dynamic disturbance, and clarified the breeding mechanism of rock burst in the mining of different types of structural coal mines. Hou Wei[25], focusing on the "C"-shaped overlying strata spatial structure, explored the laws of rock strata movement in isolated coal bodies with three mined-out sides and the rock burst disasters induced by such rock strata movement. Du Erbao et al.[26] systematically investigated the effects of initial crack defects on the stability of coal pillars under different types of composite roof structures and loading conditions, and revealed the evolution law of fracture networks in defective coal pillars and their composite roof structures. Li Jian et al.[27] employed uniaxial compression tests, scanning electron microscopy(SEM), acoustic emission(AE) and other techniques to reveal the multi-scale high-temperature deterioration mechanism of coal pillars. Li Yang et al.[28] analyzed the mechanical properties of roof strata and their fracturing characteristics, and optimized the width design of narrow coal pillars for gob-side entry retaining. Yang Yao et al.[29] combined geological data and on-site monitoring data, and adopted the methods of moment sensor inversion and stress field analysis to reveal the instability evolution process and failure mechanism of coal pillars. Fu Zhiyong et al. [30]systematically investigated the working face deformation and the safe bearing capacity of coal pillars by means of on-site monitoring and numerical simulation, and optimized the width of coal pillars between two fully mechanized working faces. Chen Dingchao et al.[31] investigated the stress distribution law and plastic zone failure characteristics of special-shaped coal pillars, and divided the coal pillars into four zones: damaged zone, progressive failure zone, stable zone, and special zone. Han Penghua et al.[32] quantitatively analyzed the effects of goaf water level height and coal pillar width on coal pillar stability.Wang Hongwei et al. [23] revealed that the main factor causing rock bursts in the working face is the sudden release of elastic strain energy accumulated in the roof during the periodic fracture of the main roof.

In terms of rock burst prevention and control, it is mainly divided into regional anti-impact and

local anti-impact according to the mining stage. Among them, regional anti-impact measures mainly avoid the formation of isolated working faces through reasonable development layout; no coal pillars are left directly in the working face or narrow coal pillars are set. For local anti-impact measures, they mainly achieve the effects of reducing the stress concentration degree of coal and rock mass, changing the physical and mechanical properties of coal and rock, and transferring the high stress concentration area to the deep part of coal and rock mass, thereby reducing the possibility of impact hazards, such as roof blasting and large-diameter drilling for pressure relief[34-36].

Due to the diversity and complexity of inducing factors for rockburst, as well as the varied and sudden nature of its manifestations, understanding the mechanisms, monitoring, and prevention of rockburst must be closely linked to the geological and mining conditions of the coal mine working face. Only then can the mystery of rockburst occurrence be unveiled, enabling targeted monitoring and prevention of potential rockburst risk zones affected by mining activities. coal seam in Shandong Mine, Eastern Mining Area, which has been subjected to multiple mining disturbances. Using a combined approach of theoretical analysis, numerical simulation, and field experiments, the research investigates the stress evolution and deformation instability mechanisms of the irregular section coal pillar under repeated mining impacts. Additionally, it proposes a rockburst prevention and control technology that integrates improving the mechanical characteristics of high and low key strata in the overlying strata with near-field large-diameter borehole pressure relief. The findings aim to provide a reference for rockburst prevention measures in section coal pillars.

2 Engineering Background

The coal mine in Shandong Province, China, has a designed production capacity of 6 million tonnes per year. The mine adopts a vertical shaft development layout within the industrial site, with a two-wing diagonal exhaust ventilation system. The primary mining target is the No. 3 coal seam, which has a thickness ranging from 8.10 m to 9.73 m, averaging 8.71 m. The seam exhibits stable thickness and a simple structure, with a dip angle of 2-16° (average 9°). The mining method employed is fully mechanized top-coal caving, utilizing longwall retreat mining with full caving for roof management. The lithological characteristics of the coal seam's roof and floor strata are presented in Table 1.

Table1 Lithological characteristics of coal seam roof and floor strata

Names of roof and floor	Names of rocks	Thickness(m)	Lithological characteristics
Roof of No.3 coal	No.2 coal	0.61	black, dominated by durain with clarain (secondarily), and belongs to a locally minable unstable coal seam with

			relatively large variations in thickness, f=2.8.
	Mudstone	2.35	grayish black, with a dense massive structure, containing aluminous materials and plant fragment fossils, and the rock is relatively fragmented, f=4.0.
	Medium-fine sandstone	13.18	light gray to grayish white, mainly composed of quartz with feldspar as the secondary component, presenting a medium-thick bedded structure. Horizontal and gently wavy bedding are well-developed. It is hard and dense, with argillo-calcareous cementation, and fractures are relatively well-developed, f=6-8.
	Siltstone	3.99	dark gray, dense and relatively hard, with argillaceous cementation, massive structure, relatively well-developed joints, and the rock is relatively fragmented, f=4-5.
No.3 coal	Coal	8.71	black, dominated by durain with clarain as the secondary component, and belongs to semi-dull coal. It has a banded texture and a layered structure, with a stable thickness, f=3.0.
Floor of No.3 coal	Silty mudstone	2.01	grayish black, with a dense massive structure; the upper part contains aluminous materials and plant fragment fossils, and the rock softens when exposed to water, f=4.0.
	Interbedded siltstone and fine sandstone	15.07	gray to light gray, hard and dense, mainly composed of fine sandstone with intercalated siltstone strips, presenting a medium-thick bedded structure; horizontal and gently wavy bedding are well-developed, with argillo-calcareous cementation and good sorting.

According to the coal and rock mechanical parameter tests, the dynamic failure time (DT), elastic energy index, impact energy index, and uniaxial compressive strength of Coal Seam 3# are 30.2ms, 3.017, 5.844kJ respectively. The bending energy indexes of the roof and floor are 108.178kJ and 93.327kJ respectively. It can be known that the impact risks of Coal Seam 3#, its roof and its floor are strong impact risk, weak impact risk and weak impact risk respectively [37]. Meanwhile, the stress relief method was adopted to carry out in-situ stress tests in the mining area. The results show that the maximum principal stress is horizontal stress, with a value of 15.62MPa, which is 1.33-1.42 times that of the vertical stress and 1.81-1.93 times that of the minimum horizontal stress, showing obvious directionality.

The No.5316 working face is located at the southern boundary of the No.5 mining area and is a to-be-mined working face. It extends westward to the designed stoping line of the working face, and its northern part, adjacent to the auxiliary transport gateway, borders the goafs of the already mined 5312, 5311, 5310, 5309, 5307 and 5306 working faces, with an isolation coal pillar of 3.5-18m reserved. The working face has a layout length of 122-244m and an advance length of 1361m, as

shown in Fig. 1.

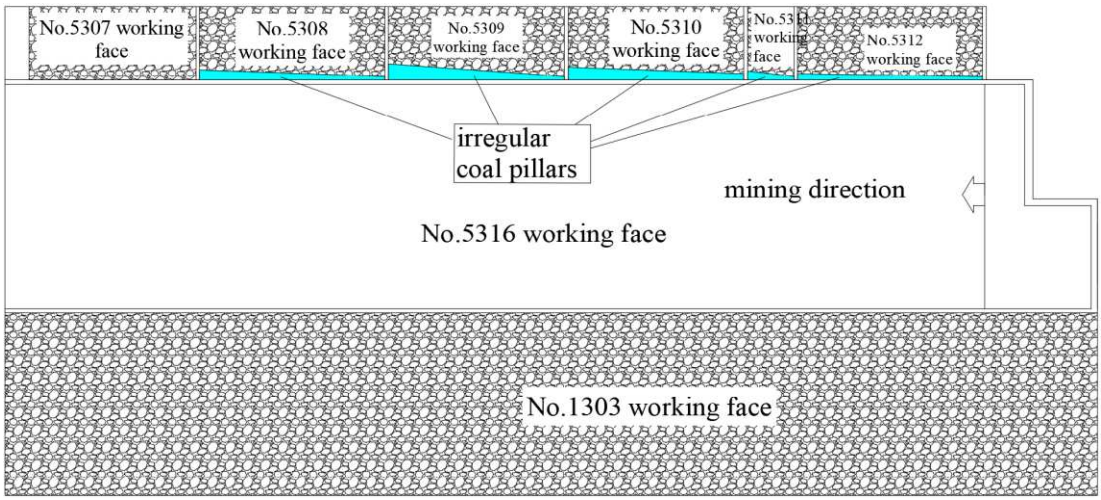

Fig.1 The layout plan of the No.5316 working face

3 Stress evolution mechanism of irregular section coal pillars under mining influence

Based on the lithological characteristics revealed by the boreholes in the working face, and by applying the mine pressure theory and key stratum theory, the step-by-step breaking process of the overlying roof's key strata at all levels in the irregular coal pillar area during the mining process of the working face under the condition of surrounding goafs is analyzed as follows:Working face mining → The low-level key stratum of medium-fine sandstone with a thickness of 4.5m, located 0.05m above the coal seam, undergoes bending, tension and breaking → The low-level key stratum loses stability by rotation and touches the gangue → The sub-low-level key stratum of siltstone with a thickness of 8.0m, located 25.06m above the coal seam, bends and breaks in tension → The sub-low-level key stratum loses stability → The high-level key stratum of fine sandstone with a thickness of 42.43m, located 67.22m above the coal seam, bends and deforms → If the high-level key stratum undergoes large-area breaking and weighting, the section coal pillar is highly likely to induce impact instability due to a significant increase in the bearing stress inside the coal pillar.

3.1 Theoretical model for stress analysis of irregular section coal pillars

The stress distribution state borne by section coal pillars varies with their width. The coal pillar load is mainly affected by two types of overlying rock structures: one is the load generated by the broken overlying rock of the upper low-level and sub-low-level key strata, and the other is the load generated by the overlying rock during the bending and subsidence process of the high-level key stratum. The stress analysis of the section coal pillar is carried out, as shown in Figure 2. F_{dn} is the

self-weight stress of the overlying rock strata on the coal pillar; F_B is the horizontal force exerted by the stable gangue in the goaf on the coal pillar; Fgn is the horizontal force exerted by the gangue in the goaf of the working face being mined on the section coal pillar, but this force increases with the rise of the height of the caving zone and the improvement of the compaction degree of the gangue in the goaf, and its magnitude is relatively small.

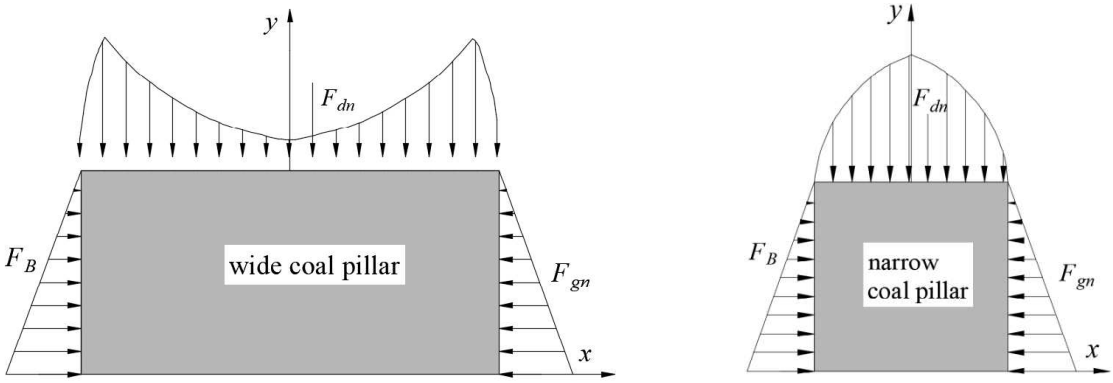

(a) wide coal pillar (b) narrow coal pillar

Fig.2 Schematic diagram of stress state analysis for section irregular coal pillars

If the coal pillar is wide enough, the coal pillar on the goaf side can be divided into a broken zone, a plastic zone, an elastic zone, and an original rock stress zone. A microsegment of the coal pillar is taken and simplified as a plane strain problem for processing. It is assumed that the coal pillar is isotropic and homogeneous, and conforms to the ideal elastoplastic softening model. The mechanical model of lateral abutment pressure is shown in Figure 3. In the figure, x_1 represents the broken zone, x_2 the plastic zone, x_0 the limit equilibrium zone, and x_3 the elastic zone. $K\gamma H$ denotes the peak stress increment acting on the interface between the coal pillar and the roof, and q_1 stands for the load of the caving zone strata above the coal pillar.

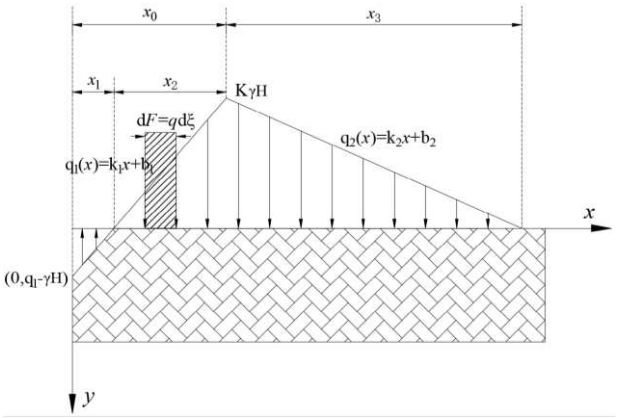

Fig.3 Analysis model of bearing capacity of wide coal pillars

By the principle of superposition, the stress components at any point M (x, y) in the coal pillar under the action of overlying loads can be obtained, as shown in Equation (1):

$$\begin{cases} d\sigma_y = -\dfrac{2q_i(x)d\xi}{\pi}\dfrac{y^3}{\left(x^2+y^2\right)^2} \\ d\sigma_x = -\dfrac{2q_i(x)d\xi}{\pi}\dfrac{x^2y}{\left(x^2+y^2\right)^2} \\ d\sigma_{xy} = -\dfrac{2q_i(x)d\xi}{\pi}\dfrac{xy^2}{\left(x^2+y^2\right)^2} \end{cases} \quad (1)$$

The width of the working face section coal pillar is irregular, so the stress state of the coal pillar is divided into wide coal pillar stress and narrow coal pillar stress for separate calculation.

(1) Stress state of wide coal pillars

If within this influence range $x_0 < \frac{1}{2}x \le$ abutment stress, there exists a stress superposition zone in the middle of the coal pillar, a mechanical model for stress superposition in the elastic zone of the wide coal pillar is established as shown in Figure 4, where the coal pillar in the stress superposition zone bears the load $Q=\sum_{i=1}^{n}\frac{E_i h_i^3 \gamma_i h_i}{E_i h_i^3}$, and the coordinate of the intersection point on the left side of the elastic zone is $\left(\frac{Q-b_2}{k_2}, Q\right)$.

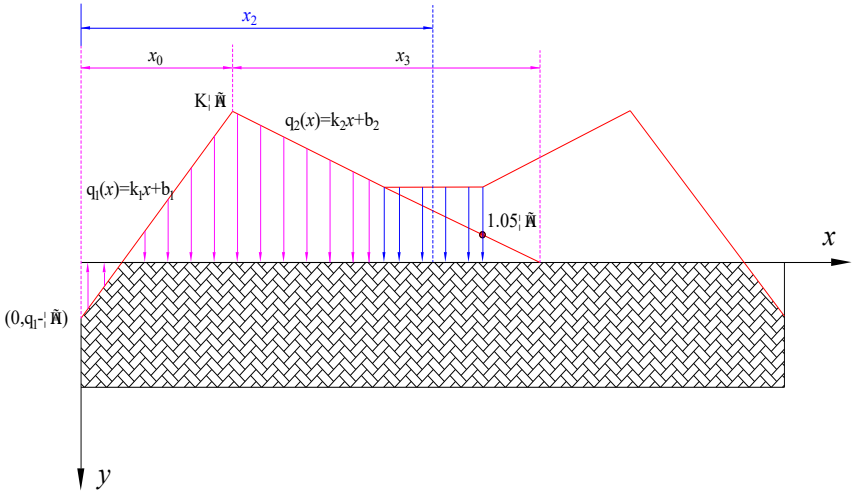

Fig.4 Mechanical model for stress superposition in the elastic zone of wide coal pillar

The expressions for the triaxial stress at any point in the wide coal pillar derived from Equation (1) are as follows:

$$\begin{cases} \sigma_y = \Delta\sigma_{y1} + \Delta\sigma_{y2} + \Delta\sigma_{y3} - \gamma H = \int_0^{x_0} -\dfrac{2(k_1\xi + b_1)y^3}{\pi\left[(x-\xi)^2 + y^2\right]^2} d\xi + \int_{x_0}^{\frac{Q-b_2}{k_2}} -\dfrac{2(k_2\xi + b_2)y^3}{\pi\left[(x-\xi)^2 + y^2\right]^2} d\xi + Q\left(\dfrac{x}{2} - \dfrac{Q-b_2}{k_2}\right) - \gamma H \\ \sigma_x = \Delta\sigma_{x1} + \Delta\sigma_{x2} - \gamma H = \int_0^{x_0} -\dfrac{2(k_1\xi + b_1)y(x-\xi)^2}{\pi\left[(x-\xi)^2 + y^2\right]^2} d\xi + \int_{x_0}^{\frac{Q-b_2}{k_2}} -\dfrac{2(k_2\xi + b_2)y^3}{\pi\left[(x-\xi)^2 + y^2\right]^2} d\xi + Q\left(\dfrac{x}{2} - \dfrac{Q-b_2}{k_2}\right) - \gamma H \\ \tau_{xy} = \Delta\tau_{xy(1)} + \Delta\tau_{xy(2)} - \gamma H = \int_0^{x_0} -\dfrac{2(k_1\xi + b_1)y^2(x-\xi)}{\pi\left[(x-\xi)^2 + y^2\right]^2} d\xi + \int_{x_0}^{\frac{Q-b_2}{k_2}} -\dfrac{2(k_2\xi + b_2)y^2(x-\xi)}{\pi\left[(x-\xi)^2 + y^2\right]^2} d\xi + Q\left(\dfrac{x}{2} - \dfrac{Q-b_2}{k_2}\right) - \gamma H \end{cases} \quad (2)$$

where $k_1 = \dfrac{(K+1)\gamma H - q_1}{x_0}$, $k_2 = \dfrac{\gamma H(1.05-K)}{x_3}$, $b_1 = q_1 - \gamma H$, $b_2 = K\gamma H - \dfrac{\gamma H x_0(1.05-K)}{x_3}$,

$x_0 = \dfrac{M(1-\sin\varphi)}{2\tan\varphi(1+\sin\varphi)} \ln\left[\dfrac{K\gamma H + \dfrac{C}{\tan\varphi}}{\left(\dfrac{C}{\tan\varphi} + P_x\right)\dfrac{1+\sin\varphi}{1-\sin\varphi}}\right]$; M is the mining height, m. C is the cohesion of the coal mass, MPa. K is the stress concentration factor. Px is the support strength, MPa.

(2) Stress state of narrow coal pillars

When x < 2x₀, the peak stresses on both sides of the coal pillar are superimposed. At this time, the distribution of lateral abutment pressure is shown in Figure 2 (b). Based on this, a mechanical model for peak stress superposition of narrow coal pillars is established as shown in Figure 5. Since the narrow coal pillar is in the limit equilibrium zone, only vertical stress acts on the interior of the coal pillar.

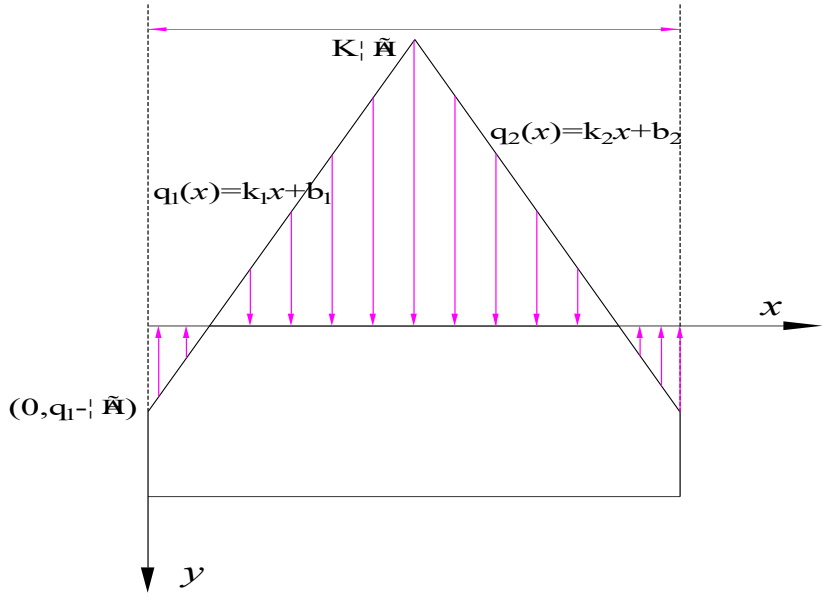

Fig.5 Mechanical model for stress superposition in the elastic zone of narrow coal pillar

Meanwhile, the expression for the vertical stress at any point in the narrow coal pillar derived from Equation (1) is as follows:

$$\sigma_y = \Delta\sigma_{y1} + \Delta\sigma_{y2} - \gamma H = \int_0^{\frac{x}{2}} -\frac{2\left(k_1\xi + b_1\right)y^3}{\pi\left[\left(x-\xi\right)^2 + y^2\right]^2}d\xi + \int_{\frac{x}{2}}^{x} -\frac{2\left(k_2\xi + b_2\right)y^3}{\pi\left[\left(x-\xi\right)^2 + y^2\right]^2}d\xi - \gamma H \quad (3)$$

where $k_1 = \frac{\gamma H - 2q_1}{x}$, $k_2 = \frac{2\left(q_1 - \gamma H - K\gamma H\right)}{x}$, $b_1 = q_1 - \gamma H$, $b_2 = \gamma H\left(2K+1\right) - q_1$。

The differential and integral equations of Equations (2) and (3) can be solved by Matlab. It can be known from the above equations that the stress magnitude at any point in the coal pillar is related to the physical and mechanical properties of the coal mass and its occurrence conditions, and is mainly affected by the size of the coal pillar itself, the stress concentration factor of the overlying rock strata, and the load of the caving zone strata.

According to the generalized Hooke's law, the calculation formula for the elastic strain energy E_1 stored in coal and rock mass under a triaxial stress state is as follows:

$$E_1 = \frac{\sigma_1^2+\sigma_2^2+\sigma_3^2-2\mu(\sigma_1\sigma_2+\sigma_1\sigma_3+\sigma_3\sigma_2)}{2E} \quad (4)$$

Where E is the elastic modulus, u is the Poisson's ratio, σ_1 is the maximum principal stress, σ_2 is the intermediate principal stress, σ_3 is the minimum principal stress.

For a coal-rock element, the principal stress expression of the Coulomb criterion is as follows:

$$\sigma_1 = \frac{1+\sin\phi}{1-\sin\phi}\sigma_3 + \frac{2c\cos\phi}{1-\sin\phi} \quad (5)$$

Where ϕ is the fault friction angle, c is the cohesion.

For a section coal pillar, its length is often much larger than its width; thus, the three-dimensional stress problem of the section coal pillar can be simplified to a plane strain problem, namely:

$$\sigma_2 = \mu\left(\sigma_1 + \sigma_3\right) \quad (6)$$

Then, by combining Eqs. (4) – (6), the ultimate elastic strain energy of the section coal pillar E_{1cr} can be expressed as a quadratic function of σ_3, and it increases with the increase of the minimum principal stress. If the section coal pillar is only subjected to the overlying rock pressure, $\sigma_3 = 0$, the ultimate elastic strain energy of the section coal pillar E_{1cr} is given by:

$$E_{1cr} = \frac{2c^2\left(1-\mu^2\right)}{E}\frac{\cos^2\phi}{\left(1-\sin\phi\right)^2} \quad (7)$$

According to Eq. (7), when the section coal pillar is only subjected to overlying rock pressure, the ultimate elastic strain energy of the section coal pillar E_{1cr} is closely related to the basic

mechanical parameters of the coal pillar.

3.2 Calculation examples of irregular coal pillars stress

Based on the mechanical test results of coal and rock mass in the No.5316 working face, the calculation example method is adopted to further study the stress evolution law of irregular section coal pillars. Taking the cohesion C as 2.45 MPa, the internal friction angle as 28°, and the roadway side support strength P_x as 0.002 MPa, and substituting them into Equations (2) and (3) for calculation, the stress distribution laws of wide and narrow coal pillars in different forms can be obtained.

(1) wide coal pillar

Using the control variable method, with the fixed breaking overlying rock action intensity q_1 = 1.45 MPa and the overlying rock stress concentration factors taking values of 2, 3, 4, 5, 6, 7, and 8, substitute them into Equation (2). The distribution curves of stress components at points in the coal pillar at different distances varying with the overlying rock stress concentration factor K, calculated by Matlab, are shown in Fig. 6.

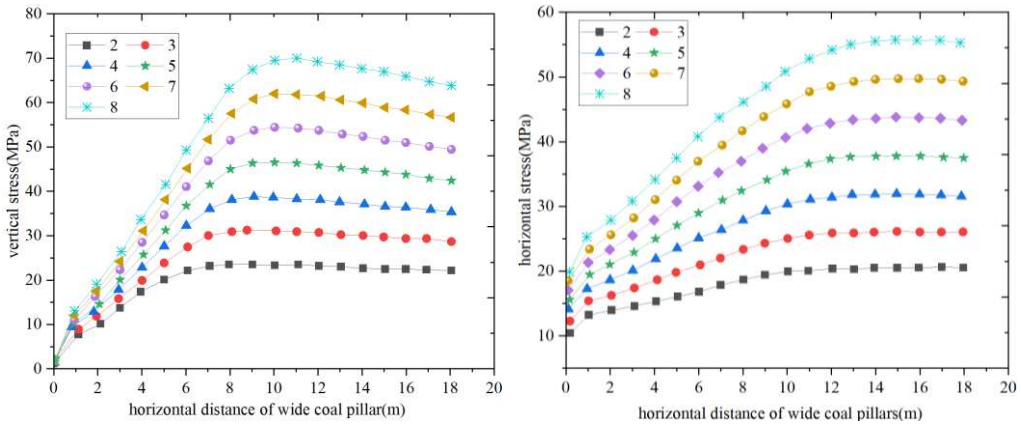

（a）vertical stress　　（b）horizontal stress

Fig.6 Evolution curves of stress in coal pillars with the increase of stress concentration factor

As analyzed from Fig. 6, with the increase of the stress concentration factor K, both the vertical stress and horizontal stress in the wide coal pillar increase, showing a relatively consistent variation trend. When the coal pillar width increases from 0m to 10m, the vertical stress in the coal pillar increases with the increase of the stress concentration factor. When the coal pillar width reaches 10m, the maximum vertical stress reaches its peak, and then gradually decreases as the coal pillar width continues to increase. At this point, the range of the limit equilibrium zone in the coal pillar expands to some extent.

(2) Narrow coal pillar

For the narrow coal pillar, with the stress concentration factors of the overlying rock strata on

the coal pillar taking values of 3, 4, 5, 6, 7, and 8, and the caving rock load of the overlying strata q_1 = 1.45 MPa, substituting them into Equation (3) and calculating with Matlab software, the distribution curves of vertical stress in the narrow coal pillar varying with the stress concentration factor are obtained, as shown in Fig. 7.

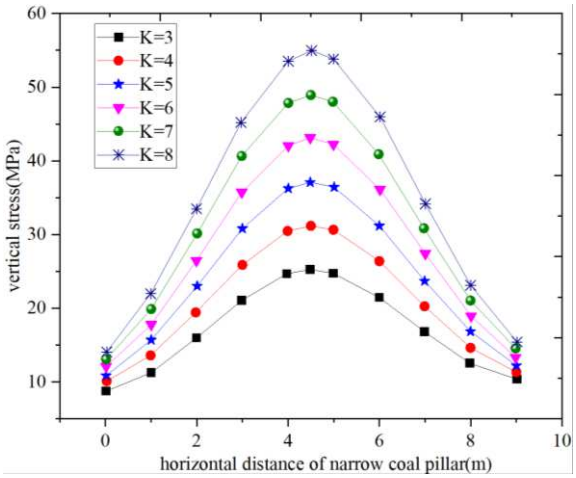

Fig.7 Distribution curves of vertical stress variation in narrow coal pillar

As analyzed from Fig. 7, the vertical stress of the narrow coal pillar increases with the increase of the overlying rock stress concentration factor. The stress increment on both sides of the narrow coal pillar is very small, while the stress increment in the middle is obvious. This indicates that both sides of the narrow coal pillar are in a broken state with low residual strength, while the interior still has strong bearing capacity. As the stress concentration degree increases, the narrow coal pillar will lose stability when the vertical stress in the middle exceeds the ultimate load strength of the coal mass.

4. Numerical Simulation Study on Stability of Irregular Section Coal Pillars

To further study the stress field and the evolution and distribution characteristics of the plastic zone in the irregular coal pillar area during the mining process of the No.5316 working face, the FLAC3D numerical calculation software is used to construct a three-dimensional numerical model of the irregular coal pillar under the mining influence area of the No.5316 working face, so as to explore the stability of the coal pillar during the working face mining process.

4.1 Model Establishment and Simulation Scheme of Irregular Coal Pillars

According to the geological and mining conditions of the No.5316 working face, irregular coal pillars with widths of 4-7m, 4-10m, 7-14m, 4-18m and 4-11m are respectively left between the auxiliary entry of the 5316 working face and the goafs of the No.5312, No.5311, No.5310, No.5309 and No.5308 working faces. After systematically analyzing the movement law of the overlying strata during the mining process of the No.5316 working face, the geometric section view of the constructed

three-dimensional model is shown in Figure 8. To simulate the influence of overlying strata fracture on the goaf side of the section coal pillar on the stability of the section coal pillar during working face mining, a simple harmonic sine stress wave is applied at the position of the main roof 10m directly above the coal pillar, with a peak stress of 5.5MPa and an action time of 0.2s (one cycle). Local damping is selected during the simulation process.

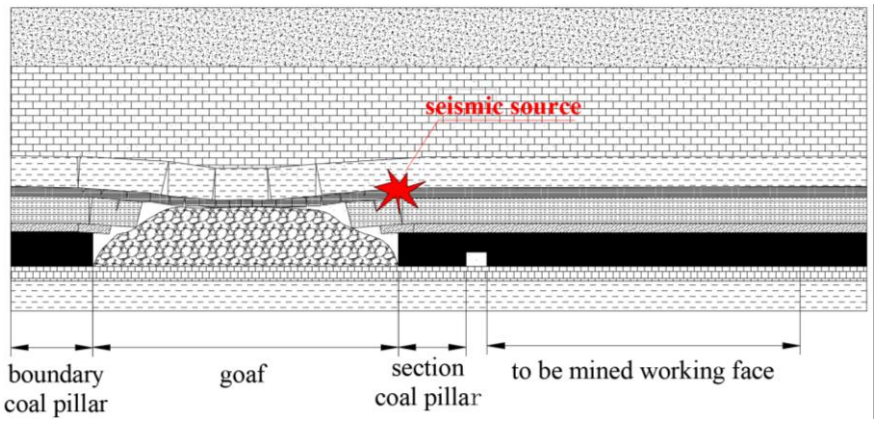

Fig.8 Geometric profile of irregular coal pillars

To focus on simulating and analyzing the stability of the irregular coal pillars in the 5316 working face, separate models were built for each coal pillar during the numerical modeling process, as shown in Fig. 1.

Based on the above modeling analysis, the specification and size of the constructed numerical model are: X×Y×Z = 1230m×600m×200m. The Y-axis of the numerical model is the layout direction of the working face, and the advancement is from the positive direction to the negative direction along the X-axis. The buried depth of the coal seam is about 436m, the gravitational acceleration is 9.8m/s^2, the average bulk density of the overlying rock strata in the model is 25kN/m^3, and the vertical load calculated according to $\sigma z = \gamma H$ is 5.5MPa. The numerical calculation model adopts the Mohr-Coulomb yield criterion, and the mechanical parameters of each coal and rock stratum are assigned according to the measured results of the test. The constructed numerical model is shown in Figure 9.

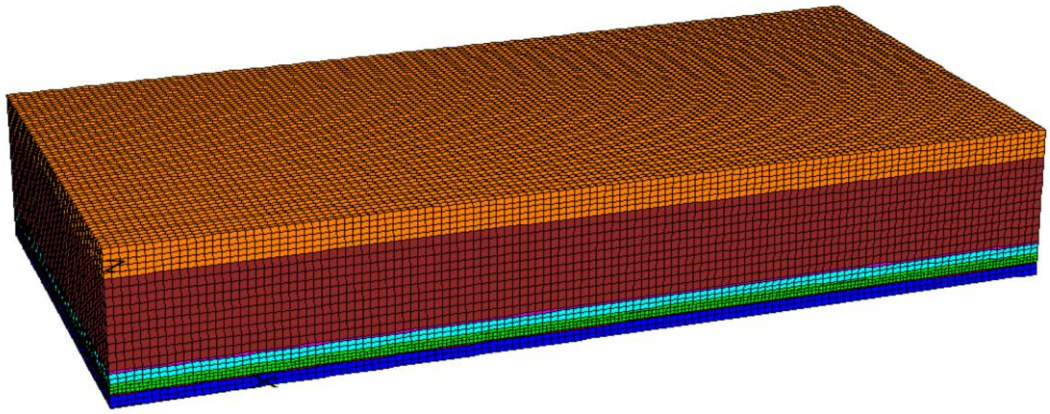

Fig.9 Three-dimensional numerical calculation model of irregular coal pillars under the mining of No.5316 working face

The purpose of this numerical simulation is to systematically analyze the stability of irregular coal pillars under the influence of working face mining by studying the evolution laws of coal pillar stress, plastic zone and its energy. According to the actual mining time sequence of the adjacent working faces of the 5316 working face, the simulation scheme is designed as follows:

(1) Initial rock stress balance;

(2) Simulating the mining of the 1303 working face;

(3) Simulating the mining of the 5308 working face;

(4) Simulating the mining of the 5309 working face;

(5) Simulating the mining of the 5310 working face;

(6) Simulating the mining of the 5307 working face;

(7) Simulating the mining of the 5311 working face;

(8) Simulating the mining of the 5312 working face;

(9) Simulating the mining of the 5316 working face;

(10) Save the data once every time the working face is mined.

During the numerical calculation process, data are saved at specific mining distances of the working face according to the distribution length of irregular coal pillars. For the convenience of analysis, data are saved respectively when the working face is mined to the range of the strike layout of the corresponding coal pillars. The specific data saving settings for each irregular coal pillar during the working face mining are shown in Table 2.

Table2 Data saving settings for numerical calculation of irregular coal pillars during working face mining

Coal pillar	coal pillar location	coal pillar	corresponding	Number of

serial number		width(m)	working face mining distance(m)	numerical calculation savings (time)
I	No.5316 auxiliary entry and No.5312 working face	4-7	124-324	4
II	No.5316 auxiliary entry and No.5311 working face	4-10	328-378	2
III	No.5316 auxiliary entry and No.5310 working face	7-14	382-572	4
IV	No.5316 auxiliary entry and NO.5309 working face	7-18	576-766	4
V	NO.5316 auxiliary entry and No.5308 working face	4-11	770-970	4

When the stope is unmined, the surrounding rock of the stope is in a state of initial rock stress balance. During the mining of the No.1303 working face, the lateral pressure of the working face acts on the No.5316 working face, causing the coal and rock mass to store a certain amount of energy. With the successive mining of the No.5308, No.5309, No.5310, No.5307, No.5311 and No.5312 working faces, the stress of the coal and rock mass in the No.5316 working face increases significantly, and the accumulated elastic energy will further increase. In particular, the stress concentration of the coal and rock mass near the auxiliary entry side of the No.5316 working face will be particularly prominent. Especially during the continuous mining process of the No.5316 working face, the stress concentration in the irregular coal pillar area will further increase, and the range of plastic failure of the coal pillar will be more serious, which is likely to induce the instability of the coal pillar.

4.2 Analysis on Stability of Irregular Coal Pillars

(1) Characteristics of Coal Pillar Stress Distribution

To facilitate the analysis of the vertical stress distribution law of irregular coal pillars during the mining process of the No.5316 working face, the vertical stress nephograms of the coal pillars are processed using two sets of saved data of the coal pillars within the mining range of the working face and the data when the working face has not yet mined to the coal pillars. The vertical stress distribution nephograms of the section and plane of each irregular coal pillar under working face mining are obtained, and the characteristics of the vertical stress distribution of the coal pillars are analyzed respectively, as shown in Figures 10 to 14.

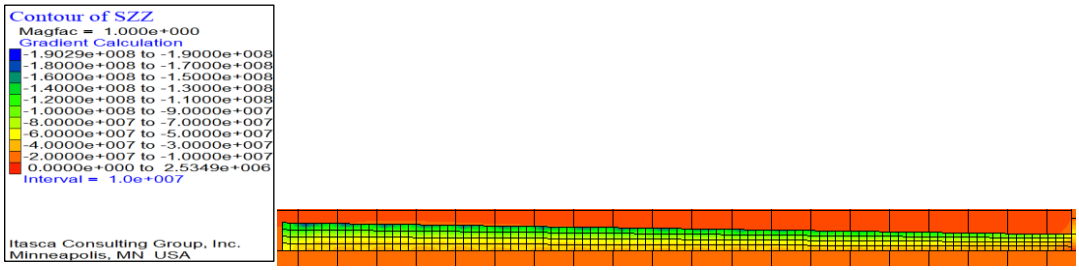

（a）working face mining 70m

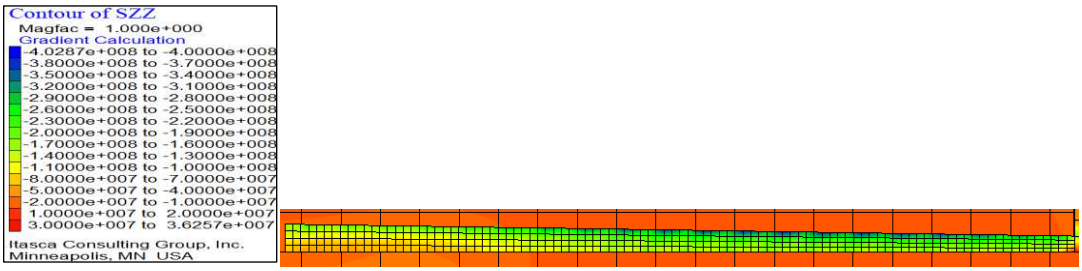

（b）working face mining 274m

Fig.10 Vertical stress of I# coal pillar during the mining process of the working face

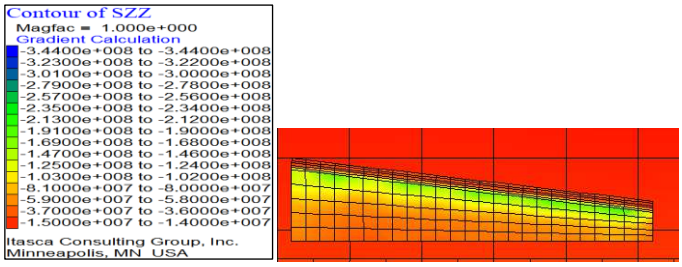

（a）working face mining 274m

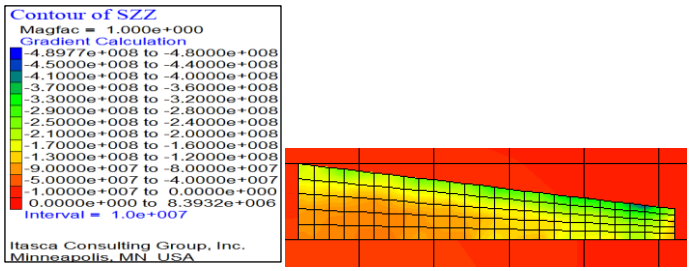

（b）working face mining 353m

Fig.11 Vertical stress of II# coal pillar during the mining process of the working face

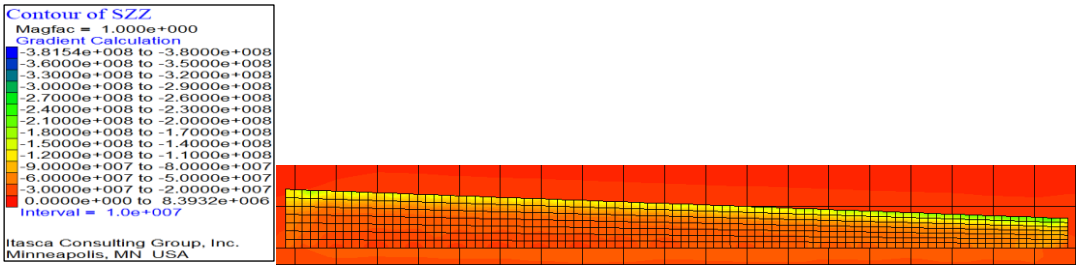

（a）working face mining 353m

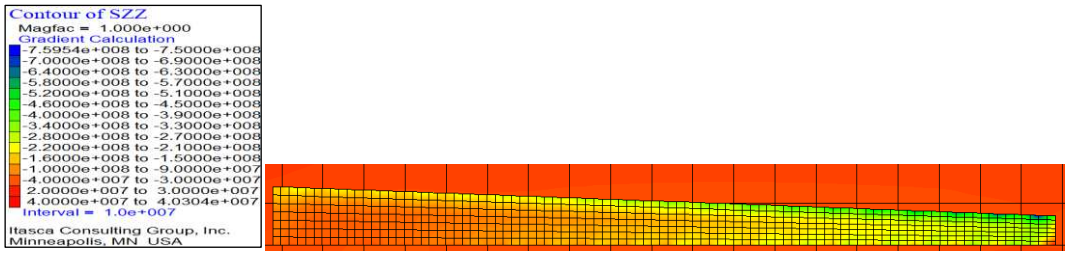

（b）working face mining 532m

Fig.12 Vertical stress of III# coal pillar during the mining process of the working face

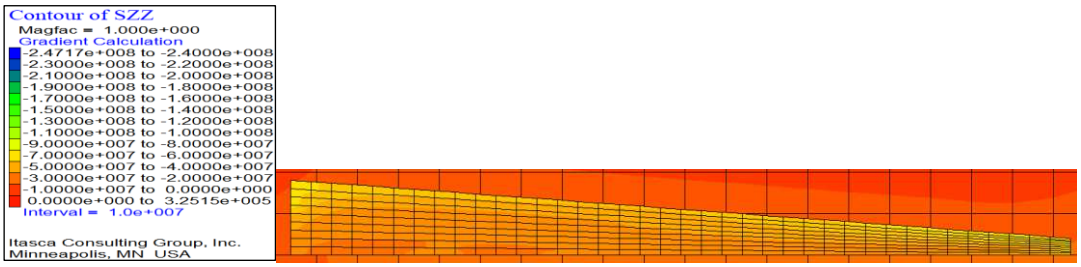

（a）working face mining 532m

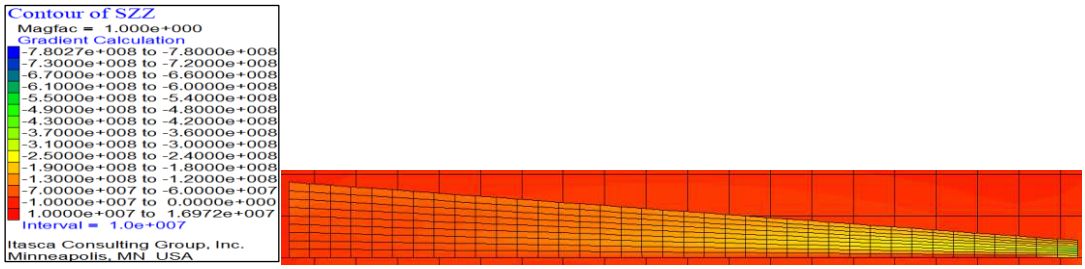

（b）working face mining 726m

Fig.13 Vertical stress of IV# coal pillar during the mining process of the working face

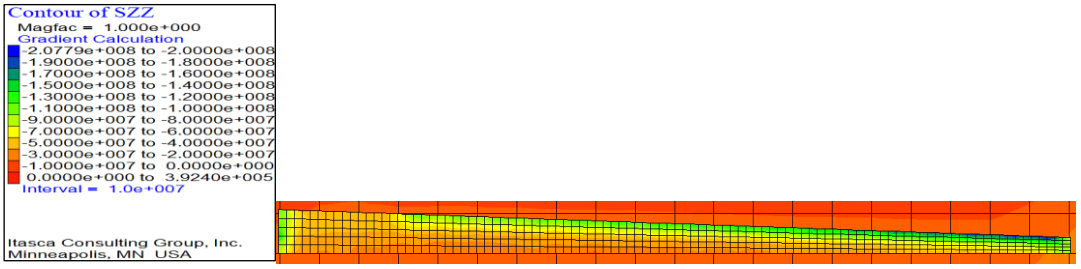

（a）working face mining 726m

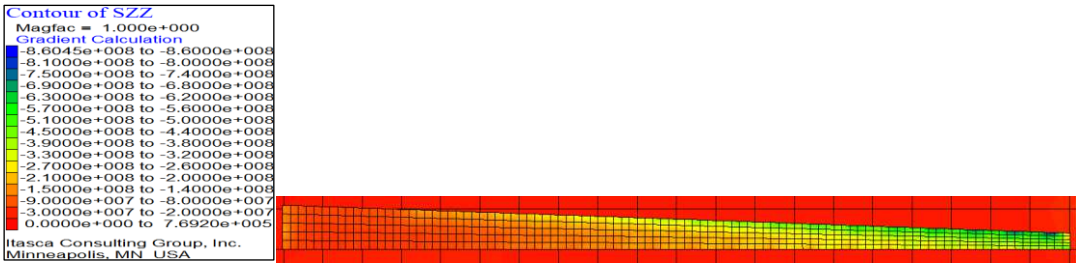

（b）working face mining 920m

Fig.14 Vertical stress of V# coal pillar during the mining process of the working face

As can be analyzed from Figures 10 to 14, during the continuous mining process of the No.5316 working face, the overall vertical stress of the irregular section coal pillars shows an increasing trend, and the vertical stress at the end of the coal pillar close to the working face and its evolution are closely related to the advancing progress and the shape of the coal pillar. During the working face mining, the vertical stresses of Coal Pillar I, II, III, IV and V increased from 22.81MPa by 53.07% to 35.06MPa, from 27.70MPa by 80.75% to 41.76MPa, from 30.30MPa by 130.17% to 69.74MPa, from 38.21MPa by 190.08% to 110.84MPa, and from 29.70MPa by 144.95% to 72.75MPa respectively. The specification and shape of coal pillars are prone to cause stress concentration. Under the coupling effect of mining and overlying strata movement in adjacent goafs, the vertical stress value in the corner areas of coal pillars will be larger, and the possibility of impact instability of coal pillars under the disturbance of far-field and near-field loads increases.

In addition, in view of the distribution characteristics of irregular coal pillars, the numerical simulation results were processed to obtain the lateral stress distribution curves in the central area of the irregular coal pillars, as shown in Figure 15.

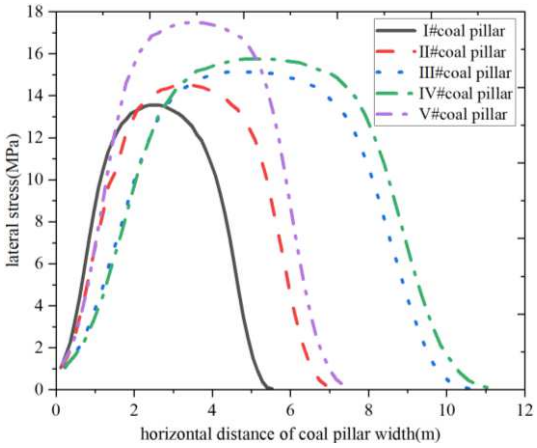

Fig.15 Lateral stress distribution of section coal pillars

As analyzed from Figure 15, the variation trend of the lateral stress of the section coal pillar in the numerical simulation results is basically consistent with that in the theoretical calculation results, both showing an "upward convex" distribution, i.e., a trend of first increasing and then decreasing. When the working face is mined to the layout area of each coal pillar, the maximum lateral stresses of Coal Pillar I, II, III, IV and V obtained by simulation calculation are 13.56MPa, 14.51MPa, 15.13MPa, 15.74MPa and 17.47MPa respectively. Moreover, the larger the width of the coal pillar, the relatively larger the bearing range of the bearing core area of the coal pillar.

(2) Energy Distribution Characteristics of Sectional Irregular Coal Pillars

Based on the results of the numerical simulation, the numerical calculation results of the stresses

in all directions are substituted into the energy formula, and the distribution of stored energy and ultimate energy of the sectional coal pillars during the working face mining process is obtained, as shown in Fig. 16.

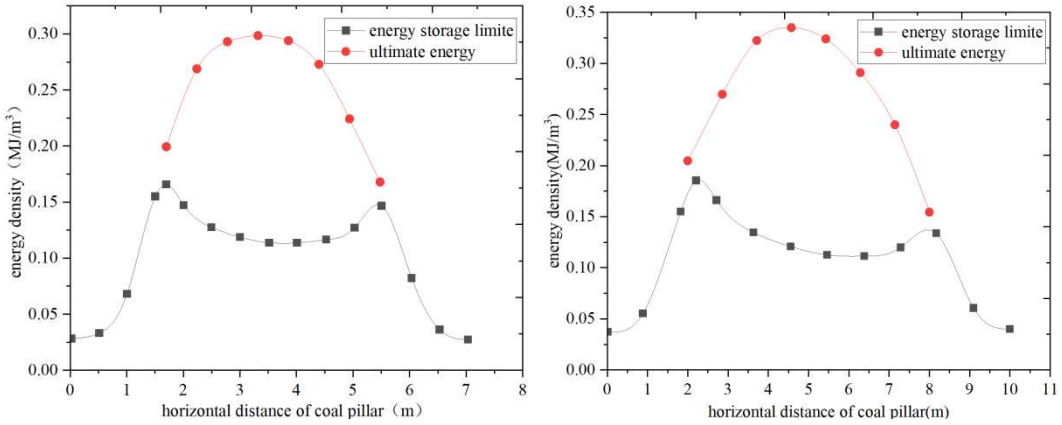

（a）I#coal pillar

（b）II#coal pillar

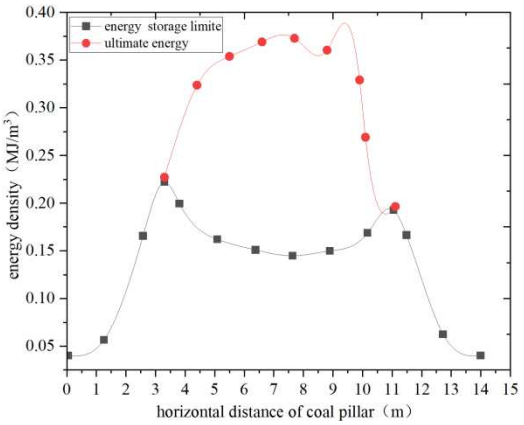

（c）III#coal pillar

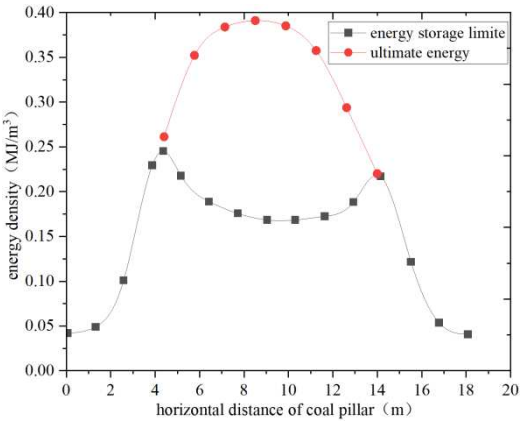

（d）IV#coal pillar

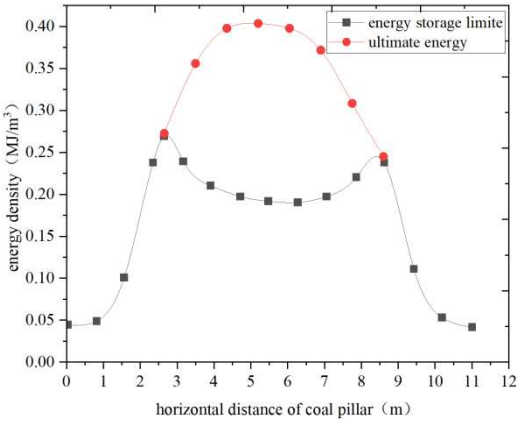

（e）V#coal pillar

Fig.16 Comparison and distribution of elastic energy and ultimate energy of section coal pillars

As can be analyzed from Fig. 16, the elastic energy density of the irregular section coal pillars in the working face presents a "bimodal" distribution. From both sides to the middle, it first increases,

then decreases, and finally tends to be stable, with the peak point located at the elastic-plastic junction. The stored energy in the elastic zone is lower than the ultimate energy, indicating that the elastic zone is relatively stable. With the continuous mining of the working face, the energy peaks on both sides gradually increase. The energy peaks on the goaf side of Coal Pillar I, II, III, IV and V are 0.147MJ/m³, 0.133MJ/m³, 0.193MJ/m³, 0.217MJ/m³ and 0.238MJ/m³ respectively, and the energy peaks on the mining side are 0.166MJ/m³, 0.185MJ/m³, 0.222MJ/m³, 0.245MJ/m³ and 0.269MJ/m³ respectively. The energy stored in the coal pillars continues to increase, and the accumulated energy provides support for the occurrence of coal pillar-type rock burst.

Based on the above research results, combined with the energy and stress distribution laws of coal pillars with different widths, it can be judged and analyzed that the main forms of the possibility of impact danger occurring in the sectional coal pillars during the working face mining process are: local instability impact of coal pillars and large - scale instability impact of coal pillars. During the continuous mining of the working face, the effective bearing width of the coal pillar is reduced more, which aggravates the lateral unloading amplitude of the elastic zone. When an impact occurs, the difference between the stored energy and the ultimate energy is larger than that in a local impact, which induces the instability of the coal mass in the deeper part of the elastic zone, making the impact more intense

5 Prevention and Control Technology for Irregular Coal Pillars Rock Burst

5.1 Assessment of Irregular Coal Pillars Rock burst Risk

For the rock burst risk assessment of irregular coal pillars, multiple monitoring methods such as microseism, online stress monitoring, and drill cuttings method can be used to capture the physical and mechanical information of the coal pillar area. These monitoring information are converted into time series, and a unified monitoring time window is set according to the data samples. Combined with monitoring logs, the impact probability reflected by various monitoring information within the monitoring window is calculated. Then, various information is fused and analyzed according to the Dempster-Shafer evidence theory to obtain a fused dynamic danger value, so as to determine the risk degree of coal pillar impact under mining influence. The calculation process is as follows.

(1) Expection rock burst of Irregular Coal Pillars

The rock burst levels are classified into No Impact (NI), Weak Impact (WI), Moderate Impact (MI), and Strong Impact (SI). Among them, Moderate impact and strong impact are regarded as early warning levels, and the expression of impact expectation P_{ME} is as follows:

$$\mathrm{P}_{ME}(\mathrm{A}) = \mathrm{P}_{ME}(\mathrm{A}/\mathrm{X}_{MI+SI}) \tag{4}$$

$$\mathrm{P}_{ME}(\mathrm{A}/\mathrm{X}_{MI+SI}) = \sum_{j=1}^{n} jP_{ME-j}(\mathrm{A}/\mathrm{X}_{MI+SI}) \tag{5}$$

where $P_{ME}(\mathrm{A}/\mathrm{X}_{MI+SI})$ is the probability of rock burst occurring at the early warning level; j is the monitoring signal of the j-th sensor; n is the number of sensors for monitoring information.

(2) Probability of coal pillar impact occurrence

According to the research, the impact hazard monitoring methods for irregular coal pillar areas include microseism, online stress monitoring, and drill cuttings method, so n is set to 3. Combining formulas (4) and (5), the impact occurrence probability M(A) in irregular coal pillar areas can be obtained as follows:

$$\begin{cases} M(\phi) = 0 \\ M(\mathrm{A}) = \prod_{id=1}^{3} M_{id}(\mathrm{A}) + \lambda \cdot \mathrm{f}(\mathrm{A}) \\ M(\overline{A}) = 1 - M(\mathrm{A}) \\ M(\mathrm{H}) = 0 \end{cases} \tag{6}$$

where $\lambda = 1 - \prod_{id=1}^{3} M_{id}(\mathrm{A}) - \prod_{id=1}^{3} \mathrm{M}_{id}(\overline{A})$, $f(\mathrm{A}) = \frac{1}{3}\sum_{id=1}^{3} M_{id}(\mathrm{A})$

(3) Coal Pillar Impact Probability Correction

Based on the data from microseismic monitoring, online stress monitoring, and the drill cuttings method, the corrected probability of coal pillar impact occurrence δ_{rs} within the same monitoring time window is as follows.

$$\delta_{rs} = (1-\xi) \times \delta_{hp} + \xi \times \Delta P_D \tag{7}$$

Where $\xi \in [0,1]$ is the correction coefficient. $\Delta P_D = \frac{1}{3}\left(\frac{\omega_2 - \omega_1}{\omega_0} + \frac{\gamma_2 - \gamma_1}{\gamma_0} + \frac{\mu_2 - \mu_1}{\mu_0}\right)$, ω_0, ω_1, ω_2 is the microseismic data obtained from monitoring within the same time window. The λ_0, λ_1, λ_2 is the online stress data obtained from monitoring within the same time window. The μ_0, μ_1, μ_2 is the drilling cuttings data obtained from monitoring within the same time window.

(4) Dynamic Early Warning Index for Coal Pillar Impact

Based on the monitoring data of irregular coal pillars, the modified probability of rock burst is adopted as the comprehensive monitoring and evaluation index for impact hazard, and the dynamic

early warning index for coal pillar impact $R_d(A)$ is determined as follows:

$$R_d(A) = \delta_{rs} / P(B) \quad (8)$$

Where is the basic probability of rock burst occurrence, $P(B) = n\Delta T / T$, n is the number of rock bursts occurring during the mining process of the mine. ΔT is the determined time window. T is the total time of monitoring data in the coal pillar area under mining influence.

Based on the dynamic early warning index for coal pillar impact, the determined classification of coal pillar impact hazard levels is shown in Table 3.

Table3 Classification table of coal pillar rock burst risk levels

hazard state	$R_d(A)$ range of values
No impact	$0 \leq R_d(A) \leq 0.5$
Weak impact	$0.5 < R_d(A) \leq 1.0$
Moderate impact	$1.0 < R_d(A) \leq 5.0$
Strong impact	$R_d(A) > 5.0$

Due to the differences in overlying rock spatial structure and coal pillar specifications and sizes in irregular coal pillar areas, in order to accurately assess their impact hazard, impact hazard assessments are conducted separately for different irregular coal pillar regions. According to the mining progress of the working face, the data time periods obtained for each irregular coal pillar region are shown in Table 4.

Table4 Time period data obtained from each irregular coal pillar area

Serial number	Area	Time period
1	Coal pillar I	2023.11.5~2024.1.31
2	Coal pillar II	2024.2.8~2024.2.29
3	Coal pillar III	2024.3.6~2024.5.15
4	Coal pillar IV	2024.5.19~2024.8.17
5	Coal pillar V	2024.8.21~2024.10.29

Based on the time period data of each coal pillar area determined in Table 3, the microseismic, stress and drilling cuttings data of each coal pillar area are counted and sorted out, and the impact probability of the coal pillar area is calculated. At the same time, as the working face continues to advance, the obtained data samples will continue to increase, and the calculated impact probability will be continuously corrected, so as to calculate the impact hazard degree of the coal pillar area. The

impact hazard levels of different coal pillar areas obtained through probability calculation are shown in Table 5.

Table5 Classification of impact hazard levels in different regular coal pillar areas

Serial Number	Rock burst probability	Rockburst risk levels
I	1.73	Moderate rock burst risk
II	0.81	Weak rockburst risk
III	0.69	Weak rockburst risk
IV	3.32	Moderate rock burst risk
V	0.94	Weak rockburst risk

5.2 Prevention and control technology for irregular coal pillar areas

For the prevention and control of rock bursts in irregular coal pillar areas, the prevention and control of coal pillar rock bursts needs to comprehensively consider the difficulty of prevention and control as well as economic benefits. A comprehensive analysis of the rock burst hazard levels in irregular coal pillar areas should be conducted, and hierarchical management should be carried out according to the hazard levels. The rock burst hazard levels can be divided into two-level prevention and control measures: preventive management and symptomatic management. A coal pillar rock burst prevention and control method that combines the optimization of the overlying rock structure of thick and hard roofs with stress control is proposed, and a set of rock burst prevention and control technology systems suitable for irregular coal pillar areas with different impact hazard levels in the 5316 working face is developed, as shown in Fig. 17.

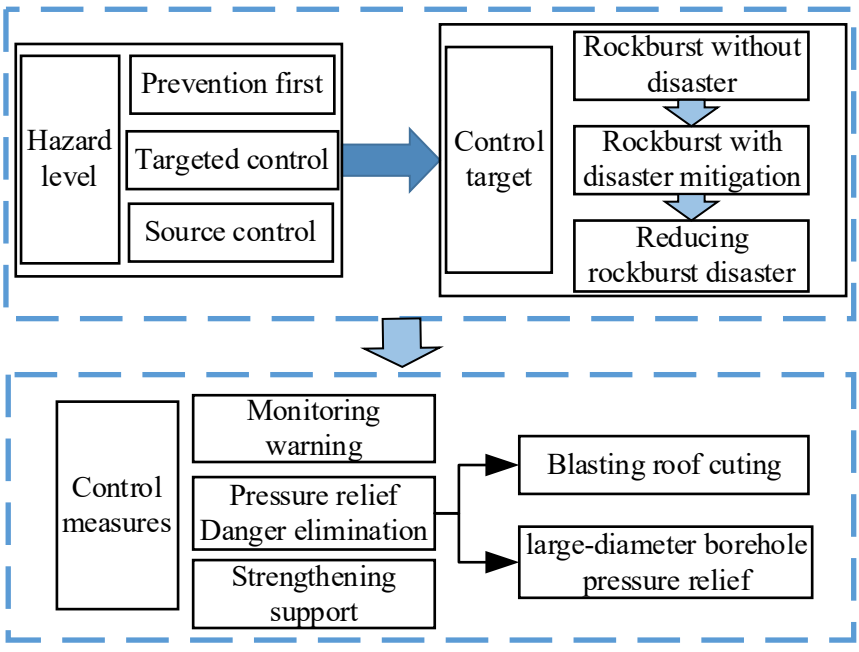

Fig.17 Prevention and control process of rock burst in irregular coal pillars

5.2.1 Prevention and control scheme for irregular coal pillars

Based on the previously determined classification of impact hazard levels for irregular coal pillars in the mining area, different prevention and control measures are adopted for the divided impact hazard zones. For zones with moderate impact hazard, a combination of roof-breaking blasting and large-diameter borehole pressure relief is used to weaken or eliminate the force source of the overlying rock structure borne by the irregular coal pillars during the mining of the working face. For zones with weak impact hazard, large-diameter borehole pressure relief measures are adopted to eliminate the possibility of impact hazard induced by mining disturbances.

5.2.1.1 Design of Roof Pre-splitting Blasting Parameters

(1) Design of Roof Pre-splitting Blasting Parameters

In view of the medium impact hazard area, in order to ensure the timely fracture of the roof of the irregular coal pillar in the auxiliary haulage roadway of the working face, it is necessary to carry out roof pre-splitting blasting for pressure relief in the auxiliary haulage roadway of the working face. Based on the geological conditions, mining technical conditions and the drilling equipment of the mine, the determined roof blasting parameters are as follows:

a. Blasting borehole diameter

Considering the hole-forming capacity of the drill bit and the construction experience of adjacent working faces in the mine, the diameter of the pre-splitting blasting hole is determined to be 75mm.

b. Determination of blasthole spacing

To avoid large-area hanging roofs in the goaf behind the working face and ensure that the fractures formed after roof pre-splitting blasting can be interconnected as a whole, according to relevant theories of rock mechanics, the calculation formulas for the radii of the blasting crushing zone and fracture zone inside the rock mass are as follows:

$$R_c = \left[\frac{\rho_0 D_v^2 n K^{-2\eta} l_c B}{8\sqrt{2}\sigma_{cd}} \right]^{\frac{1}{\alpha}} r_b \tag{9}$$

$$R_p = \left[\frac{\sigma_{cd}}{\sigma_{td}} \right]^{\frac{1}{\beta}} \left[\frac{\rho_0 D_v n K^{-2\eta} l_e B}{8\sqrt{2}\sigma_{cd}} \right]^{\frac{1}{\alpha}} r_b \tag{10}$$

Where D_V is the detonation velocity of coal, m/s. ρ_0 is detonation velocity of coal explosive kg/m^3;

n is the pressure increase coefficient, generally taken as $n=10$; $K=d_b/d_c$ is radial decoupling coefficient; l_c is axial charge coefficient,take $l_c=1;d_b,d_c$ is the blasthole radius and the cartridge radius, mm; η is the expansion adiabatic index, generally taken as 3; σ_{td} a is the dynamic tensile strength of rock，MPa； σ_{cd} is the dynamic compressive strength of rock,MPa.

By substituting the mechanical parameters of the relevant coal and rock masses in the working face into (Equation 9) and (Equation 10) for calculation to estimate the size of the affected area after blasting, the final results show that the radius of the crushing zone (Rc) is approximately 0.15~0.3m, and the radius of the fracture zone (Rp) is approximately 4.8m. Considering the original parameters for blasting roof cutting in the mine, the designed spacing of blasting roof cutting boreholes is 15m.

c.Determination of roof cutting angle

Comprehensively analyzing the specific construction conditions of the working face, the mechanical properties of the roof rock, and referring to the roof cutting schemes of adjacent working faces, the preliminary construction angles for the roof pre-splitting blasting boreholes are determined as elevation angles of 50°, 60°, and 70°.

d. Determination of roof cutting height

Based on the comprehensive stratigraphic column of the No.5316 working face, the main roof consists of a medium-fine sandstone layer with an average thickness of 13.18 m, which is the target layer for roof pre-splitting blasting as its thickness exceeds 10 m. Therefore, the designed roof cutting height should penetrate this sandstone layer entirely.

The 5316 working face has an average coal seam thickness of 8.71 m, with an immediate roof of siltstone 3.99 m thick, and the roadway height is calculated at an average of 4 m. Thus, the minimum roof cutting height is: H=8.71-4+3.99+13.18=21.88 m. To ensure the construction effect and enable the pre-split surface formed by pre-splitting blasting to completely penetrate this medium-fine sandstone layer, the preliminary designed roof cutting heights are 22 m, 24 m, and 26 m.

(2) Determination of pressure relief parameters for roof pre-splitting blasting

For the numerical simulation of roof pre-splitting blasting, the FLAC3D finite element simulation software is used to explore the influence law of roof pre-splitting blasting pressure relief on the stress distribution of surrounding rock in the auxiliary haulage roadway of the No.5316 working face. According to relevant theories of rock mechanics, it is calculated that the radius of the blasting crushing zone affected by blasting (Rc) is approximately 0.15~0.3m, and the radius of the

fracture zone (Rp) is 4.8m. In the FLAC model, a spherical area is established to equivalently replace the area affected by blasting (with a spherical radius of 5m). The grid is divided using Griddle software. The model has a length of 600m, a width of 560m, and a height of 250m. The rock mass constitutive relation adopts the Mohr-Coulomb model. The established numerical calculation model is shown in Figure 18.

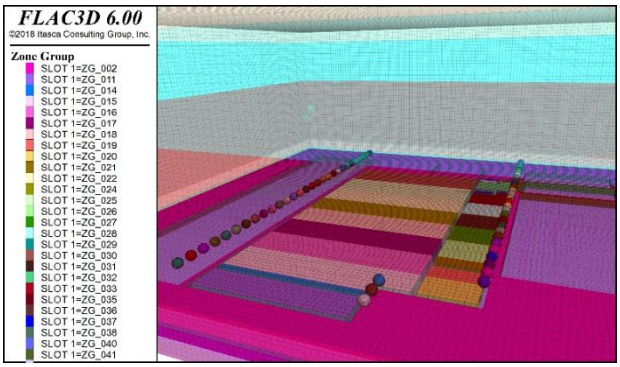

Fig.18 Schematic diagram of the numerical model

a. Roof pre-splitting blasting angle

The fixed variable method is adopted. In the numerical model, the roof cutting height is set to 22 m, and the pre-splitting blasting angles of 50°, 60°, and 70° are simulated respectively. The influence of the blasting hole angle on the pre-splitting blasting effect is compared and analyzed to determine the optimal blasting borehole angle. Through simulation, the stress distribution curves of the surrounding rock in the auxiliary haulage roadway of the working face under the influence of different roof cutting angles are obtained, as shown in Fig. 19.

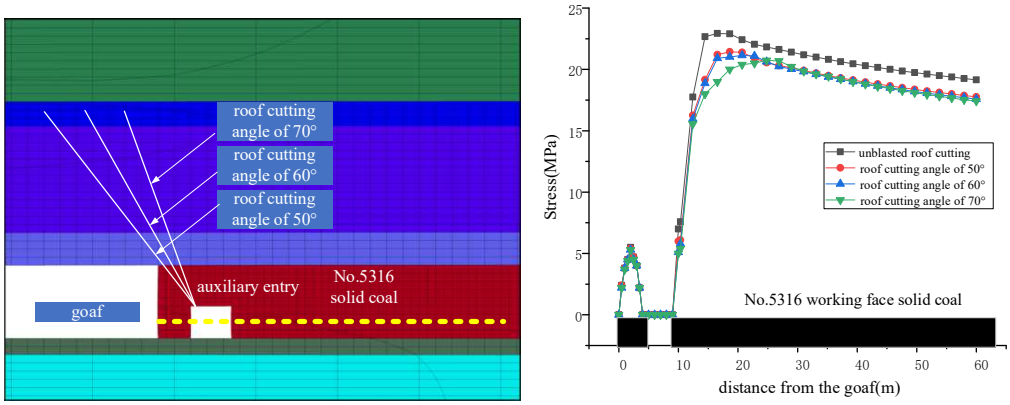

（a） （b）

Fig.19 Curve diagram of stress distribution in surrounding rock of auxiliary entry under different roof cutting angles

It can be analyzed from Figure 19 that as the angle of the roof blasting borehole increases, the peak stress of the surrounding rock on the solid coal side gradually shifts to the deep part, and the

peak stress gradually decreases, with the internal stress of the coal pillar remaining at a low level. When the borehole angle is 70°, the peak stress is 14 m away from the roadway, with a peak stress value of 20.7 MPa. At this point, the peak stress on the solid coal side is the farthest from the coal wall and has the smallest peak value, indicating the best pressure relief effect of roof blasting.

b. Roof pre-splitting blasting cutting height

In the numerical model, the blasting borehole angle is set to 70°, and simulations are conducted for blasting roof cutting heights of 22m, 24m, and 26m respectively. The influence of the blasting roof cutting height on the pre-splitting blasting effect is compared and analyzed to determine the optimal blasting roof cutting height. The stress distribution curves of the surrounding rock in the auxiliary haulage roadway under the influence of different roof cutting heights obtained from the simulation are shown in Figure 20.

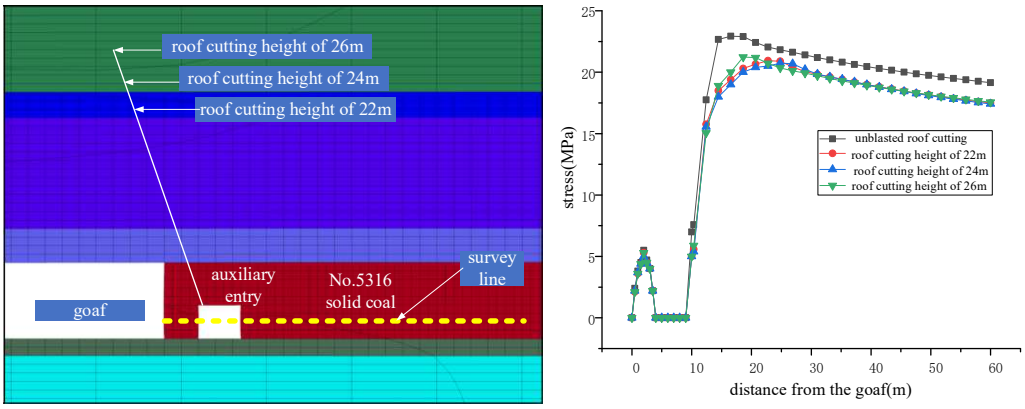

（a） （b）

Fig.20 stress distribution curves in surrounding rock of auxiliary entry under different roof cutting heights

It can be analyzed from Figure 20 that as the height of the roof pre-splitting hole increases, the peak stress of the surrounding rock on the solid coal side gradually shifts to the deep part of the coal mass, and the peak stress first decreases and then slightly increases. When the roof pre-splitting height is 24m, the peak stress on the solid coal side is the farthest from the coal wall with the smallest peak value, and the peak stress of the roof is also the smallest, which is more conducive to roadway maintenance, indicating the best effect at this time.

In summary, the on-site roof pre-splitting blasting parameters for the working face are determined as follows: the blasting borehole angle is 70°±5°, the borehole depth is 24m, the borehole diameter is 75mm, the charge length is 12m, and the charge quantity per hole is not less than 27kg.

5.2.1.2 Design of pressure relief parameters for large-diameter boreholes

While implementing the auxiliary haulage roadway blasting roof cutting measures, large-

diameter pressure relief boreholes are constructed in the mining coal rib of the auxiliary haulage roadway. The pressure relief boreholes have a diameter of 150mm, a depth of 25m, and a spacing of 2m. The distance from the boreholes to the roadway floor is 0.5-1.5m, and the boreholes are perpendicular to the coal rib. The advance distance of the pre-pressure relief boreholes is not less than 250m. The layout of the pressure relief boreholes is shown in Figure 21.

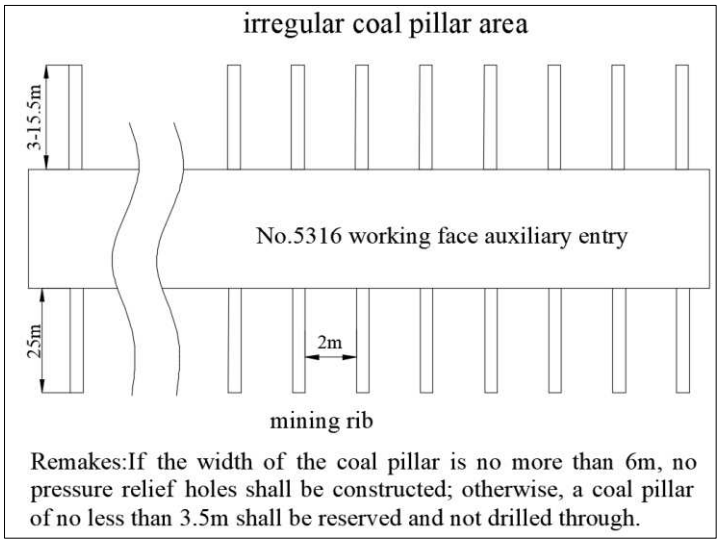

（a）

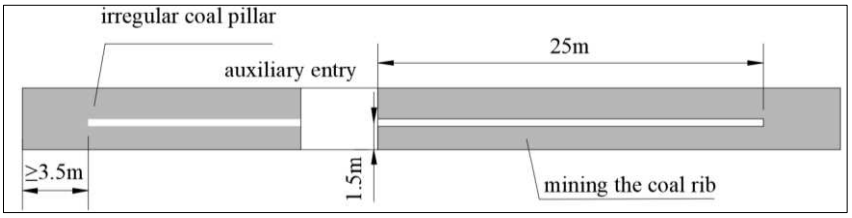

（b）

Fig.21 layout of large-diameter pressure relief boreholes

Numerical simulation analysis shows that the pressure relief effect of large-diameter boreholes is significant, with the maximum vertical stress reduced to 16.74 MPa. After the construction of large-diameter pressure relief boreholes, the plastic range of the roadway rib is effectively expanded, forming an effective pressure relief area, which reduces the possibility of rock burst in irregular coal pillars under mining disturbance.

5.2.2 Prevention and control effect of irregular coal pillars

(1) Results of on-line stress monitoring

After the implementation of rock burst prevention and control measures, the on-line stress monitoring of the irregular coal pillar area in the working face has always maintained a monitoring range of over 200m. For stress gauges in areas with weak or no rock burst risk, they are arranged in

groups with a spacing of no more than 30m; in areas with moderate rock burst risk, the group spacing is no more than 20m. Each group is equipped with two stress sensors, with burial depths of 8m and 14m respectively, and the spacing between measuring points in each group is no more than 2m. Considering the actual situation of the working face, the initial stress value for the on-line stress monitoring setup is set to be no less than 5MPa and no more than 6MPa. The layout of the on-line stress monitoring is shown in Fig. 22.

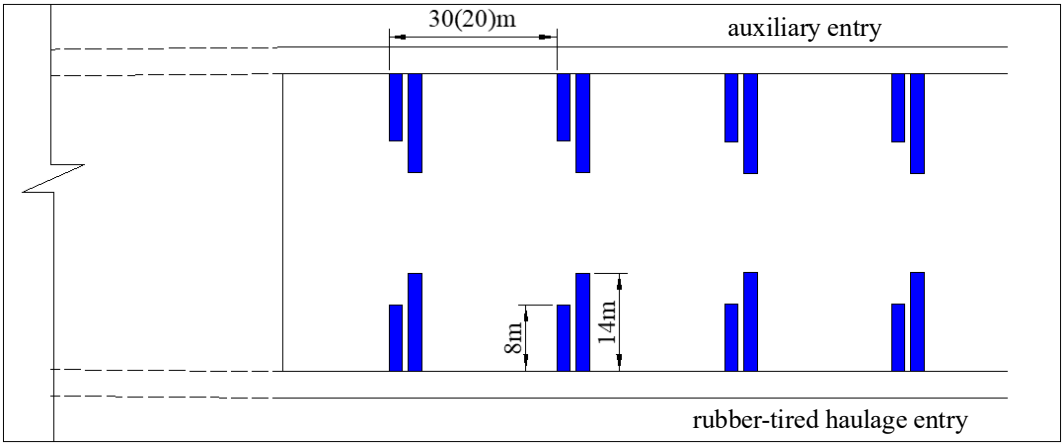

Fig.22 Schematic diagram of stress online monitoring system layout

The eight measuring points in the auxiliary haulage roadway of the working face are selected for data analysis to explore the effect of impact prevention and pressure relief, and the on-line stress monitoring data distribution curve as shown in Fig. 23 is plotted.

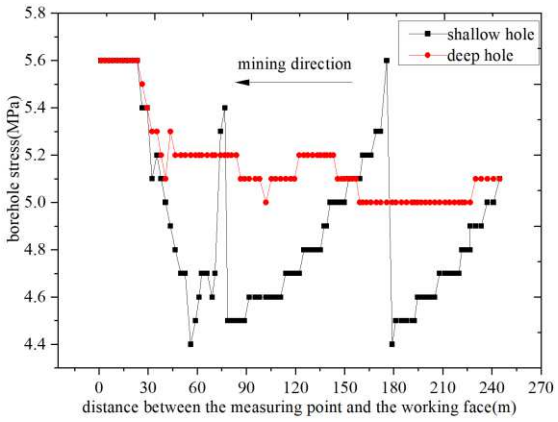

（a）113#265 measuring point

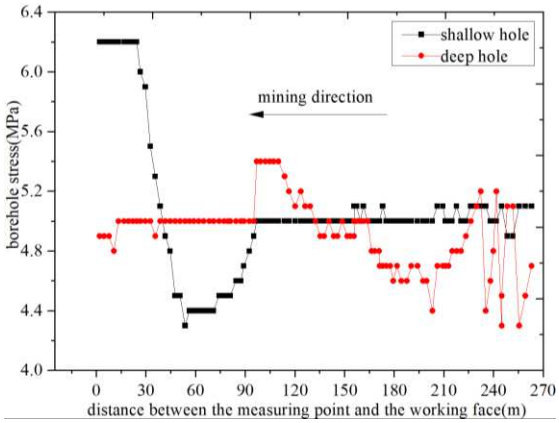

（b）114#283 measuring point

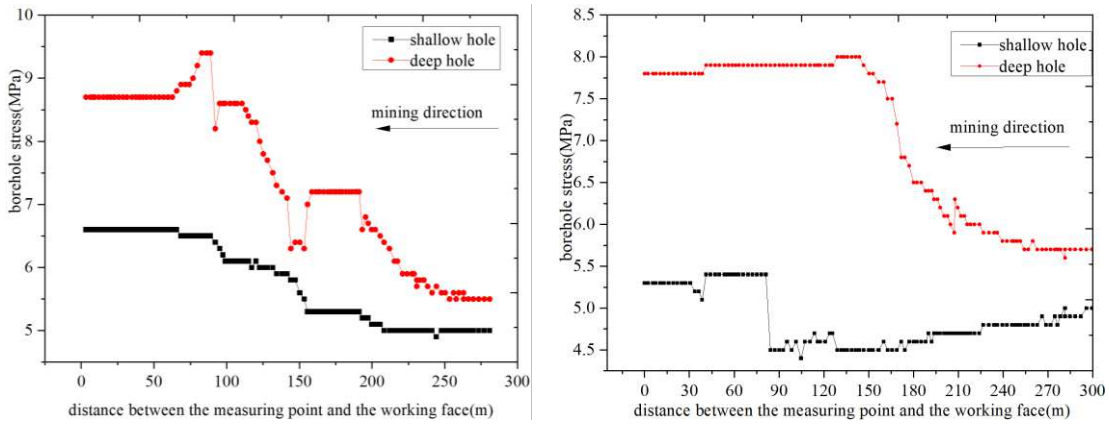

（c）115#301 measuring point　　（d）116#318 measuring point

Fig.23 distribution curves of auxiliary entry boreholes stress under pressure relief measures

It can be analyzed from Fig. 23 that after the implementation of impact prevention and control measures in the irregular coal pillar area, during the mining process of the working face, the stress in the auxiliary haulage roadway boreholes of the irregular coal pillar shows an overall trend of slow increase as the distance between the working face and the monitoring points decreases. The borehole stress reaches the maximum when the distance from the working face is within the range of 30m-50m. Among them, the maximum stress values of the shallow and deep holes at measuring points 113#265, 114#283, 115#301, and 116#318 are: 5.6MPa and 5.6MPa, 6.2MPa and 5.4MPa, 6.6MPa and 9.4MPa, 5.4MPa and 8.0MPa, respectively, all of which are less than the impact risk early warning stress values (the stress early warning values for shallow and deep holes are 12MPa and 15MPa, respectively). Meanwhile, the maximum increase in stress of deep holes and shallow holes at each measuring point is less than 1.0MPa/d, which is less than the impact risk early warning stress increase value of 4.0MPa. No abnormal stress conditions have occurred, ensuring the safe and efficient mining of the working face.

(2) Analysis of hydraulic support monitoring data

By analyzing the periodic weighting step and weighting intensity after pressure relief, the treatment effect of roof pre-splitting blasting pressure relief measures on the roof breaking step is judged. Figure 22 shows the variation of the average end-of-cycle resistance distribution curves of the supports in the head, middle, and tail areas during the normal advancement of 224.1m to 280.8m after the implementation of pressure relief measures in the 5316 working face.

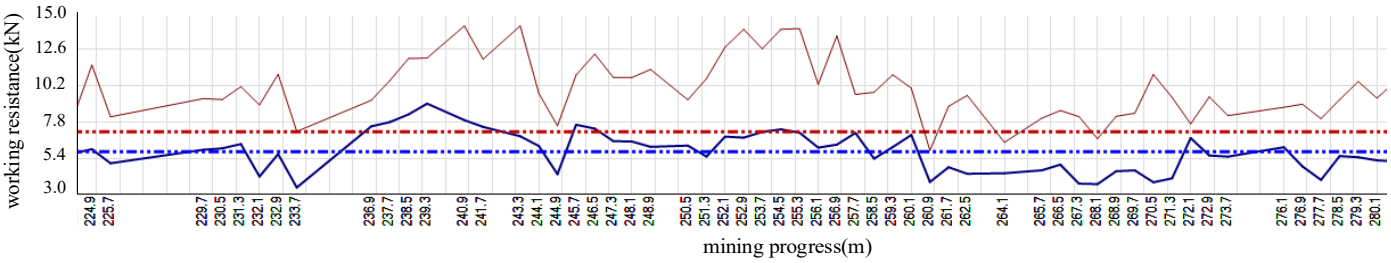

（a）machine head area（1-20#support）

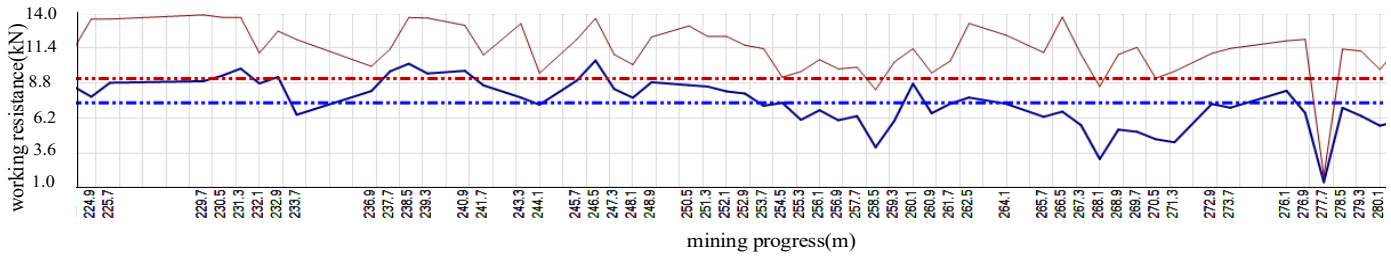

（b）middle area (supports 21#-40#support)

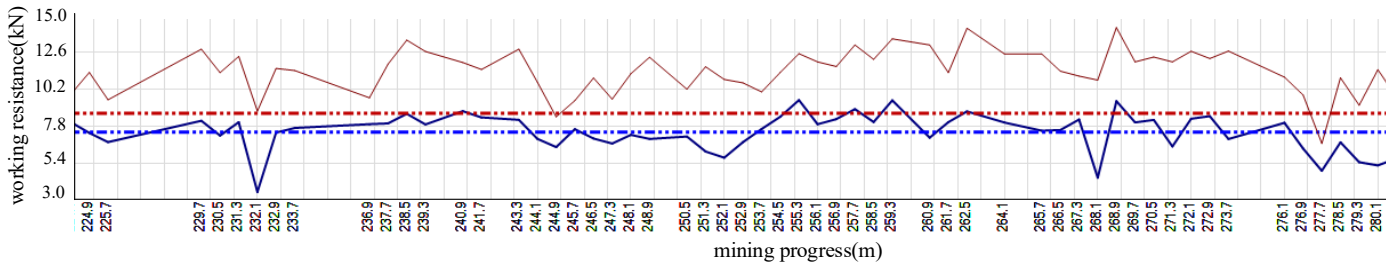

(c) Tail area (supports 141#-163#support)

Fig. 24 Support pressure data after pressure relief

As can be seen from the analysis of Fig. 24, after the implementation of roof pre-splitting blasting for pressure relief, the periodic weighting step of the roof ranges from 18.4 m to 44.0 m, with an average of 29.2 m. The end-of-cycle resistance of the working face supports is 5488-7254 kN, with an average of 6126 kN, accounting for 46-60% of the rated working resistance (12000 kN), with an average of 51.05%. During weighting, the end-of-cycle resistance of the working face supports is 7826-8721 kN, with an average of 8279 kN, accounting for 65-73% of the rated working resistance (12000 kN), with an average of 68.99%. Through calculation, the dynamic load coefficient in the monitoring area of the 5316 working face is 1.1-1.6, with an average of 1.4, and the intensity of periodic weighting is mitigated, indicating that the implemented roof pre-splitting blasting for pressure relief has achieved a good prevention and control effect.

6 Conclusions

(1) Based on the geological conditions of irregular coal pillars and the mining situation of adjacent working faces, this study analyzed the overlying strata movement and the superimposed stress distribution state of coal pillars formed by mining superposition when coal pillars of different widths are affected by secondary mining. Furthermore, based on the masonry beam theory, the expressions of vertical stress and horizontal stress borne by coal pillars of different widths were derived. By means of calculation examples, the variation law of stress in coal pillars of different widths along the width direction with the increase of stress concentration factor under mining conditions was obtained.

(2) Based on the formulated numerical simulation scheme, the evolution laws of stress and energy distribution in the irregular coal pillar area under the influence of working face mining were simulated and studied. The vertical stress and energy of irregular coal pillars #I, #II, #III, #IV and #V all showed an increasing trend. Moreover, due to the irregular shape of the coal pillars, there were differences in the stress increase in different regions of the coal pillars. Combined with the energy and stress distribution laws of coal pillars with different widths, the main forms of possibility of impact hazards occurring in the section coal pillars during the working face mining process were analyzed and judged.

(3) Considering that the occurrence of rock burst disasters has temporal and spatial dimensional characteristics, an overall evaluation method for coal pillar impact hazard is proposed, which includes microseismic monitoring, online stress monitoring and drill cuttings method monitoring information. Based on the Dempster-Shafer evidence theory, the monitoring data information in the same time window is integrally fused to obtain real-time dynamic early warning of the coal pillar area. The early warning values are 1.73, 0.81, 0.69, 3.32 and 0.94 in sequence, and their corresponding impact risks are: medium impact risk, weak impact risk, weak impact risk, medium impact risk and weak impact risk.

(4) In view of the characteristics of the impact hazard area of irregular coal pillars, a coal pillar rock burst prevention and control method that integrates the optimization of overlying strata structure of thick hard roof and stress control is proposed. Combined with the hard roof structure of the working face, the shape of irregular coal pillars, and the high stress distribution state of the surrounding rock of the auxiliary roadway, a comprehensive prevention and control technology combining "roof pre-splitting blasting and large-diameter drilling for pressure relief" has been developed. Specifically, for coal pillars with medium impact hazard, the combined prevention and control measures of roof pre-

splitting to break the roof and large-diameter drilling for pressure relief are adopted; for coal pillars with weak impact hazard, the pressure relief measure of large-diameter drilling is used. The results of on-site industrial tests show that after the implementation of the comprehensive prevention and control measures, there are no abnormal situations in stress and working resistance of hydraulic supports during the mining process of the working face, the pressure relief effect is significant, and the safe and efficient mining of the working face with thick hard roof is guaranteed.

Fundings

This work is supported by the Shandong Provincial Natural Science Foundation of China (No. ZR2018MEE009), the National Natural Science Foundation of China (52304005), the National Natural Science Foundation of Chongqing Province (CSTB2023NSCQ-MSX0016), the Special Project of the Sichuan Bureau of Geology and Mineral Resources (Sichuan Geo-Bureau, Grant No. SCDZ-DH202507), the General Project of the Anhui Engineering Research Center for Development and Utilization of Closed/Abandoned Mine Resources (Grant No. H20241221), the Horizontal Research Project of Mianyang Qimingxing Phosphorus Chemical Co., Ltd (Contract No. H20251723), and the Natural Science Foundation Project of Shandong Province (No. ZR2023ME147). The authors express sincere thanks to the reviewers for their helpful comments and suggestions for improving this paper.

Data availability

All data generated or analyzed during this study are included in this published article and its Supplementary Information files. Additional raw data (e.g., microseismic monitoring records, online stress monitoring time-series, and drill cuttings measurement data) are available from the corresponding author upon reasonable request.

Declarations

The authors declare no competing interests.

References

[1] Liu Feng, Cao Wenjun, Zhang Jianming, et al. Current technological innovation and development direction of the 14th Five-Year Plan period in China coal industry. Journal of China Coal Society, 2021, 46(01): 1-15.

[2] Xie Heping, Ren Shihua, Xie Yachen, et al. Development opportunities of the coal industry towards the goal of carbon neutrality. Journal of China Coal Society, 2021, 46(07): 2197-2211.

[3] Qi Fuzhou. Study on the Deformation Mechanism and Control of Surrounding Rock with Roof Cutting and Pressure Releasing in High Stress Roadway Driving along Next Goaf. China University of Mining and Technology, 2020.

[4] Zhang heng. Study on the law of the movement and fracture of isolated island working face ovenburden. Master's thesis, Shandong University of Science and Technology, 2004.
[5] Yu Hui. Study on the movement of upper strata and the pressure behavior law of close distance seams. Phd thesis, China University of Mining & Technology, Beijing, 2015.
[6] Xi Zhiyuan. Study on the overlying strata movement characterstics and strata behavior regularity of the island fully mechanized coal mining face. Master's thesis, Henan Polytechnic University, 2015.
[7] Jiang Fuxing. Viewpoint of spatial structures of overlying strata and its application in coal mine. Journal of Mining and Safety Engineering, 2006(01): 30-33.
[8] Dou Linming, He Hu. Study of OX-F-T spatial structure evolution of overlying strata in coal mines. Chinese Journal of Rock Mechanics and Engineering
[9] Cao Yongmo, Hua Xinzhu, Yang Ke, et al. Research on the laws of strata behavior in the Gob-side entry of the island mining face. Safety in Coal Mines, 2013, 44(01): 43-46.
[10] Ren Xing. Breaking law of overlying rock in fully mechanized caving island working face and control technology of surrounding rock in stope. Coal Engineering, 2020, 52(S1): 133-138.
[11] Qian D, Zhang N, Shimada H, et al. Stability of goaf-side entry driving in 800-m-deep island longwall coal face in underground coal mine. Arabian Journal of Geoences, 2016, 9(1): 1-28.
[12] Zhu S, Yu F, Jiang F, et al. Mechanism and risk assessment of overall-instability-induced rockbursts in deep island longwall panels. International Journal of Rock Mechanics and Mining Sciences, 2018, 106: 342-349.
[13] Manoj N B, Petros V. Fatigue and dynamic energy behavior of rock subjected to cyclical loading[J]. International Journal of Rock Mechanics and Mining Sciences, 2009, 46: 200-209.
[14] Wang Chen, Tu Hongsheng, Bai Qingsheng. Strata behavior laws of isolated short wall coal pillar fully Mechanized Caving face, Coal Safety, 2013, (10): 27-29.
[15] Zhang Xiufeng, Chen Yang. Research on the type and occurrence mechanism and prevention of coal pillar rock-bursts. Coal Science and Technology, 023,51(10): 1-11.
[16] Xianfeng Shi. Control dynamic disaster in extra thick coal seams under complex conditions. Phd thesis, University of Science and Technology Beijing, 2017.
[17] Cui Tiejun, Li Shasha, Wang Laigui. On the mesoscopic process rock burst based on the dynamic theory, Journal of Safety and Environment, 2018, 18(02): 474-480.
[18] Feng G, Wang P, Chugh Y P. Stability of gate roads next to an irregular yield pillar: a case study. Rock Mechanics and Rock Engineering, 2019, 52(8).
[19] Wang Q, Gao H, Jiang B, et al. Research on reasonable coal pillar width of roadway driven along goaf in deep mine. Arabian Journal of Geosciences, 2017, 10(21).
[20] Zhang Y, Feng G, Zhang M. Residual coal exploitation and its impact on sustainable development of the coal industry in China. Energy Policy, 2016, 96.
[21] Guo J, Feng G, Wang P. Roof strata behavior and support resistance determination for ultra-thick longwall top coal caving panel: a case study of the tashan coal mine. Energies, 2018, 11(5).
[22] Duan H, Zhao L. Prevention technology for strong mine pressure disaster in the hard-roof large-mining-height working face. Shock and Vibration, 2020, 2020(12): 1-15.
[23] Dou Linming, He Jiang, Cao Anye, et al. Rock burst prevention methods based on theory of dynamic and static combined load induced in coal mine. Journal of China Coal Society, 2015,40(7): 1469-1476.
[24] Li Xibing, Gong Fengqiang, Wang Shaofeng, et al. Coupled static-dynamic loading mechanical mechanism and dynamic criterion of rockburst in deep hard rock mines. Chinese Journal of Rock Mechanics and Engineering, 2019, 38(04): 708-723.
[25] Hou Wei, Huo Haiying. Stope rock movement rule of C-shaped of overlying strata spatial structure and disaster-causing mechanism of dynamic pressure. Journal of China Coal Society, 2012, 37(S2): 269-274.
[26] Du Erbao, Zhou Xiaoping, Zhou Nan. Numerical simulation study on the failure characteristics of the combined

structure of residual coal pillar and roof in room and pillar mining method. Engineering Failure Analysis, 2025, 174, 109531.

[27] Li Jian, Bai Jinwen, Feng Guorui, et al. Degradation mechanism of coal pillars in an underground coal gasification environment: Bearing capacity, pyrolysis behaviour and pore structure. International Journal of Mining Science and Technology, 2025, 35(6): 897-912.

[28] Li Yang, Shi Xiaoming, Wang Yuliang, et al. Optimized design of narrow coal pillars under hard roof and inclined seam conditions based on fracture behavior and stability analysis. Bulletin of Engineering Geology and the Environment, 2025, 84: 484.

[29] Yang Yao, Cao Anye, Liu Yaoqi, et al. Failure mechanism of a coal pillar with gradually decreasing width revealed by moment tensor inversion and stress field analysis. 2026.

[30] Fu Zhiyong, Zhang Wei. Research on stress change and deformation monitoring of coal pillar between two longwall coal faces. Rock Mechanics and Rock Engineering, 2024, 57(4): 2763-2772.

[31] Chen Dingchao, Wang Xianyu, Zhang Feiteng, et al. Study on the mechanism of progressive instability of special-shaped coal pillar and the stability control of roadway under the influence of mining. Rock Mechanics and Rock Engineering, 2024, 57(8): 1-23.

[32] Han Penghua, Zhang Cun, Wang Wei. Failure analysis of coal pillars and gateroads in longwall faces under the mining -water invasion coupling effect. Engineering Failure Analysis, 2022, 131. Suppl C, 105912.

[33] Wang Hongwei, Jiang Yaodong, Zhao Yixin, et al. Investigation on Mechanism of Energy Explosion During Extraction of Island Longwall Panel. Chinese Journal of Rock Mechanics and Engineering, 2013, 32(11): 2250-2257.

[34] Zhu Feng. Study on the Characteristics of shock and instability of isolated panel and rockburst prevention by liquid CO_2 cracking. Phd thesis, Liaoning Technical University, 2017.

[35] Ju Wenjun, Sun Liuwei, Liu Shahong, et al. Idea and implementation of “stress relief-support reinforcement” coop-erative control in rockburst roadway. Coal Science and Technology, 2021, 49(4): 90-94.

[36] Pan Junfeng, Yan Yaodong, Ma Hongyuan, et al. Using 300mm diameter boreholes for coal burst prevention a case study. Journal of Mining and Strata Control Engineering, 2022, 4(5):053013.

[37] GB/T 25217.2-2010 Classification and laboratory test method on bursting liability of coal. Beijing: Standards Press of China.